TOWARDS PROGRAMMABLE MATERIALS – TUNABLE MATERIAL PROPERTIES THROUGH FEEDBACK CONTROL OF CONDUCTING POLYMERS

N. S. Wiedenman*
Uniformed Army Scientist and Engineer Program, Massachusetts Institute of Technology
Cambridge, MA, 02139

I. W. Hunter
Massachusetts Institute of Technology
Cambridge, MA, 02139

ABSTRACT

This work is focused on developing an integrated device, called a *programmable material*, which mirrors the capabilities of natural co-fabricated controlled actuation systems such as muscle. While such a device may have the external appearance of a homogeneous material, it can possess unique properties not existing in any manufactured material. When actuation, sensing, and control capabilities are integrated within a closed-loop system, the mechanical properties of the system such as stiffness, viscosity, and inertia will arise from the dynamics of the feedback loop rather than from any inherent mechanical properties of the materials from which the device was fabricated. Moreover, these properties may be 'tuned' by altering the feedback parameters embedded in the material system. With this approach properties such as negative stiffness may be generated which do not exist in bulk materials.

1. INTRODUCTION

The human body contains many actuation reflex loops which enable human motion and locomotion. Through the microscopic integration of muscle fibers (actin and myosin filaments), energy delivery and waste removal systems (blood vessels), sensory mechanisms (muscle spindles and Golgi tendon organs), and control capability (nervous system), these reflex loops enable finely controllable motion.

No passive material could hope to match the performance of this system. Passive engineering materials are limited by their intrinsic properties, dictated at the atomic and molecular level. Characteristics like inertia, stiffness, and damping which determine the material's response to a mechanical input can only be changed by processing the material.

To replicate the controllable properties of muscle, an active material is required – really an integrated device. It must include an actuator component, along with sensing capability and a control system to read the sensor and drive the actuator to some desired force or position.

Beyond incorporating all the elements of a servomechanism, skeletal muscle has the further advantage of being co-fabricated. That is, the various capabilities are fully integrated at the microscopic level to the extent that muscle appears to be a single homogeneous material.

A device that can replicate these characteristics is called a *programmable material*. The actuator needed to implement an integrated co-fabricated programmable material is one without moving parts - in fact, one that comprises the material itself.

The most promising of the existing artificial muscle technologies is actuation with *conducting polymer* (CP). Of these artificial muscle technologies, conducting polymers exhibit the combination of total strain, strain rate, and low power which best match skeletal muscle (J. Madden et al., 2004). CP's have achieved good strains at low power inputs. The strain rate is still lower than desired, but has improved over recent years and continues to increase. Finally, CP's have no real moving parts. The entire material swells and contracts under the proper electrochemical conditions, so this technology was ideal for the programmable material application.

Since the goal is to create a device that externally appears to be a homogeneous material, the sensor and control electronics components were also fabricated from polymeric materials.

Such an integrated feedback device has never been fabricated in any previous research. Many researchers have fabricated various components of such a system, and have achieved significant advances in the capabilities of these individual components. This work establishes the feasibility of building the device and answers many of the questions of fabrication and design.

2. POLYPYRROLE ELECTROCHEMISTRY AND ACTUATION

In this work, the CP polypyrrole (PPy) has been used extensively. Understanding the electrochemical mechanism of deposition and actuation in PPy is vital to understanding the programmable material.

Report Documentation Page

Form Approved
OMB No. 0704-0188

1. REPORT DATE	2. REPORT TYPE	3. DATES COVERED
DEC 2008	**N/A**	**-**

4. TITLE AND SUBTITLE	5a. CONTRACT NUMBER
Towards Programmable Materials Tunable Material Properties Through Feedback Control Of Conducting Polymers	5b. GRANT NUMBER
	5c. PROGRAM ELEMENT NUMBER
6. AUTHOR(S)	5d. PROJECT NUMBER
	5e. TASK NUMBER
	5f. WORK UNIT NUMBER
7. PERFORMING ORGANIZATION NAME(S) AND ADDRESS(ES) **Uniformed Army Scientist and Engineer Program, Massachusetts Institute of Technology Cambridge, MA, 02139**	8. PERFORMING ORGANIZATION REPORT NUMBER
9. SPONSORING/MONITORING AGENCY NAME(S) AND ADDRESS(ES)	10. SPONSOR/MONITOR'S ACRONYM(S)
	11. SPONSOR/MONITOR'S REPORT NUMBER(S)

12. DISTRIBUTION/AVAILABILITY STATEMENT
Approved for public release, distribution unlimited

13. SUPPLEMENTARY NOTES
See also ADM002187. Proceedings of the Army Science Conference (26th) Held in Orlando, Florida on 1-4 December 2008, The original document contains color images.

14. ABSTRACT

15. SUBJECT TERMS

16. SECURITY CLASSIFICATION OF:			17. LIMITATION OF ABSTRACT	18. NUMBER OF PAGES	19a. NAME OF RESPONSIBLE PERSON
a. REPORT	b. ABSTRACT	c. THIS PAGE			
unclassified	**unclassified**	**unclassified**	**UU**	**8**	

2.1 Electrochemistry

The electrochemical process used to produce PPy results in a free-standing film that is mechanically robust and electrically conductive. The electrochemical deposition process was developed originally by Yamaura (Yamaura et al., 1988) and refined in the MIT BioInstrumentation Lab by John Madden, Peter Madden, and Patrick Anquetil (J. Madden, 2000; P. Madden et al., 2001; P. Madden 2003)

Electrochemical deposition of PPy is accomplished via the construction of an electrochemical cell. A solution is mixed consisting of 0.05 M pyrrole monomer (distilled and maintained at -20°C under nitrogen atmosphere protected from light), 0.05 M tetrabutylammonium hexafluorophosphate (TBAP), and 1% distilled water in propylene carbonate (PC). This solution serves as the electrolyte for the cell, which is constructed with concentric electrodes. The working electrode and deposition target consists of a glassy carbon crucible, and the counter electrode used is a polished copper sheet.

The deposition is completed at -40°C to control the rate of polymerization. After allowing the temperature to equalize, the film is deposited galvanostatically using a current density of 1.5 $\frac{A}{m^2}$ for 8-15 hours. Depositions using this technique result in films with thicknesses from 10 to 30 μm. These films have been optimized for mechanical robustness and the ability to reliably actuate for long periods of time.

Functional actuation of PPy is achieved in an electrochemical environment very similar to that used for deposition. An electrolyte solution (using propylene carbonate, water, or some other solvent) containing a salt is needed to provide dopant ions and the medium through which the ions move. The actuation environment may be the same as the deposition environment (minus the monomer), though in many cases it is beneficial to use different ions to optimize actuation behavior.

2.2 Actuation Model

The relationship between the voltage input and the strain output of the actuator is necessary in order to model the overall system behavior. The voltage output from the control electronics is an amplification of the error between the desired strain of the actuator (given by the overall system input as a voltage) and the actual strain (transduced to a voltage by the sensor). This voltage is then used as the driving input of the actuator.

John Madden (J. Madden, 2000a) derived an admittance model of a PPy actuator, called the Diffusive-Elastic-Metal (DEM) model. The DEM model was based on the fact that the PPy actuator acts as a distributed capacitance, and uses a transmission line model to represent this. The actuator admittance is then stated as,

$$Y(s)\cdot R = s\cdot\frac{\frac{\sqrt{D}}{\delta}\cdot\tanh\left(\frac{a}{2}\sqrt{\frac{s}{D}}\right)+\sqrt{s}}{\frac{\sqrt{s}}{RC}+s^{3/2}+\frac{\sqrt{D}}{\delta}\cdot s\cdot\tanh\left(\frac{a}{2}\sqrt{\frac{s}{D}}\right)}, \qquad (1)$$

where $\boldsymbol{D}$ is the diffusion coefficient, $\boldsymbol{\delta}$ is the thickness of the capacitive double layer formed at the surface of the polymer, $\boldsymbol{C}$ is the double layer capacitance, $\boldsymbol{R}$ is the polymer resistance, $\boldsymbol{a}$ is the polymer thickness, and $\boldsymbol{s}$ is the Laplace variable.

2.3 Functional Polypyrrole Actuators

Many researchers have created actuators using PPy. By manipulating deposition and actuation system variables, they have been able to increase the total strain achievable, while improving strain rate and total force. Novel actuator geometries have been developed to amplify strain and force.

The simplest PPy actuator geometry is linear (or uniaxial). Films deposited using the conditions described above normally actuate with 2-4% linear strain (Pytel, 2007).

Modifications to the deposition electrochemistry and the actuation environment can produce significantly higher strains (Hara et al., 2006). Among the highest strains achieved and sustained over many cycles was 14% (Anquetil et al., 2004).

In order to amplify the strain provided by a PPy actuator, many researchers have used a bimorph geometry, consisting of one layer of CP bonded to a second layer of passive (non-actuating) material. The passive layer serves as something for the CP to 'push off' against - that is, when the CP expands due to ion influx, the bilayer bends towards the passive layer. When the CP contracts, the bilayer bends towards the polymer layer.

However, the bilayer geometry requires a counter electrode placed near the actuator in order to complete the electrochemical circuit. This type of actuator also must be immersed in electrolyte solution, precluding use in air.

In order to amplify the strain provided by a PPy actuator, many researchers have used a trilayer. The simplest trilayer consists of two CP films separated by a passive thin electronic insulator. These two layers actuate in tandem - that is, when one CP layer expands due to ion influx the other contracts due to an opposite applied potential. The trilayer bends towards the contracting layer. When the electronic insulator layer also serves as an ionic transport layer, the trilayer can be operated in out of an electrolyte bath (P. Madden et al., 2003; Chen, 2006).

2.4 Actuation in the Programmable Material

In the current work, a uniaxial actuation geometry is visualized as the basic mode of the programmable material. In this configuration, the device consists of a single actuation layer with one surface open to an

electrolyte and counter electrode. The opposite surface of the actuator is coated with a barrier material before the sensor and control electronics layers are deposited.

As discussed above, the Madden DEM admittance model relates the input voltage to the current into the actuator. By integrating this we get the charge injected into the actuator, which we can then relate to the linear strain. By defining a strain to charge ratio, α, and further assuming that α is independent of load (J. Madden, 2000), Madden found that the relationship

$$\varepsilon = \rho\alpha\,, \tag{2}$$

gives a typical value of α for PPy of $500\times10^{-12}\ \frac{m^3}{C}$. Since the charge density $\rho = \frac{q}{V}$, where q is charge and V is the polymer volume, the overall strain resulting from actuation under loaded conditions is

$$\varepsilon = \frac{\alpha q}{LWh} + \frac{\sigma}{E}\,, \tag{3}$$

where L, W, and h are the length, width, and thickness of the polymer actuator, respectively, σ is the applied stress, and E is the polymer Young's modulus. This equation is used to represent the actuator performance under uniaxial stress conditions.

The linear configuration is useful for controlling the apparent stiffness of the programmable material. However, the system can also be used as a position-controlled device. To get useful displacements, the small strains of the actuator must be amplified through a different configuration. As mentioned previously, an excellent and simple configuration for accomplishing this is the trilayer.

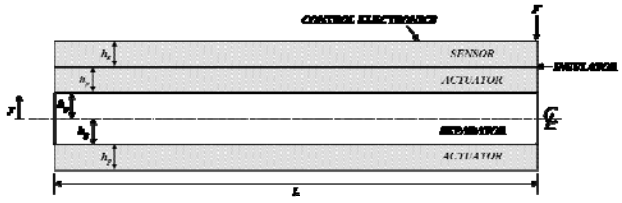

Figure 1. *This design for a programmable material is based on a trilayer actuator device. The control electronics and insulator layers are two orders of magnitude thinner than the actuator and sensor layers, and can be neglected in the elastic beam analysis of the device. Diagram based on (P. Madden et al., 2003).*

In making a trilayer-based programmable material, one of the two actuator layers in the trilayer will have the sensor and control electronics deposited on its outside surface, as shown in Figure 1. The relationship between the charge density in the PPy actuators and the resulting curvature (κ) of the device is given by

$$\frac{\kappa}{\rho} = -\frac{3\alpha}{h_g}\left[\frac{\left(1+\frac{h_p}{h_g}\right)^2 - 1}{\left(1+\frac{h_p}{h_g}+\frac{h_s}{h_g}\right)^3 + \left(1+\frac{h_p}{h_g}\right)^2 + 2\left(\frac{E_g}{E_p}-1\right)}\right], \tag{4}$$

where h_g is half the thickness of the ionic transport layer, h_p is the thickness of the actuator layer, h_s is the thickness of the sensor layer, E_g is the Young's modulus of the ionic transport layer, and E_p is the Young's modulus of the PPy actuator and sensor layers (Wiedenman, 2008).

3. SENSING

The second important component of the programmable material's feedback system is the position sensor. In order to control the actuator, it is essential that we are able to sense the actuator's resultant strain. This is accomplished by means of a strain gage, which converts the mechanical displacement of the actuator into an electrical signal usable by the control electronics to drive the actuator.

In order to accurately control the device, the viscoelastic properties of the PPy strain gage must be understood. Therefore, a study was undertaken to model the creep behavior of the sensor that will then be incorporated into the integrated system model to account for these effects.

Using a dynamic mechanical analyzer (DMA) originally designed and built by Nate Vandesteeg (Vandesteeg, 2007), it was determined that the viscoelastic behavior of the PPy sensor layer was satisfactorily modeled using a Generalized Maxwell model consisting of two parallel Standard Linear Solid model elements (Wiedenman, 2008).

Further experiments were conducted using the Vandesteeg DMA to determine the relationship between strain and resistance in the sensor. A Poisson model was proposed and experimentally verified which gives the relationship as

$$R_s = R_c\frac{1+\varepsilon_x}{\left(1-\upsilon\varepsilon_x\right)^2}\,, \tag{5}$$

where R_s is the variable sensor resistance, R_c is the unstrained sensor resistance, ν is the Poisson's ratio for PPy, and ε_x is the uniaxial strain. This sensor serves as one leg of a full Wheatstone bridge in order to generate a voltage output that is usable by the control electronics.

4. DEPOSITION AND PATTERNING OF CONTROL ELECTRONICS

The key component of a programmable material is the feedback loop embedded within it. This loop requires the fabrication of electronic components from polymeric materials that can be co-fabricated with the sensor and actuator elements. This co-fabrication requirement severely restricts the choice of fabrication techniques.

There are a limited number of methods by which a CP can be deposited. The techniques for patterning the CP control electronics are closely related to the deposition method, so these were examined simultaneously. There were several requirements that a method had to satisfy in order to be deemed appropriate for this work.

First, the fabrication of the control electronics could not damage the actuator or sensor components. Co-fabrication of the integrated programmable material requires patterned CP deposition onto a flexible and somewhat fragile CP-based substrate. If either the deposition process or the patterning technique (to include pattern removal) damages the underlying CP, the method was unacceptable.

Second, it is important to keep the overall size of the device small. Since the speed of actuation in PPy is diffusion-limited, it is important to keep the dimension normal to the electrolyte interface (usually the thickness) very small while maintaining mechanical robustness. To prevent significant ohmic losses within the actuator, which results in thermal loading of the actuator and uneven actuation (Vandesteeg, 2007), it is important to keep the width and length of the device small. This limits the available footprint upon which the electronics may be fabricated, and therefore limits the complexity of the control implementation.

Third, the technique or techniques chosen must allow deposition of both conducting and non-conducing polymer layers, or there must be a complementary method for non-conducting polymer deposition. The non-conducting layers will serve as electronic and ionic insulators between the actuator, sensor, and electronics layers.

Fourth, the deposition process should be as simple and robust as possible. Since the goal is to create a programmable material consisting completely of conducting and non-conducting polymers, silicon or metal substrates were avoided. Further, a deposition method and accompanying patterning technique with fewer variables allows for easier optimization.

Finally, the deposition technique must be capable of depositing CP onto a non-conductive substrate. This is important to allow adequate electronic isolation between the functional layers of the device.

As mentioned above, it would be self-defeating to use a fabrication process to create the control electronics which damaged the underlying CP components (i.e. sensor and actuator). This eliminates standard photolithographic techniques, as the photoresist developer damages PPy (Smela, 1999).

There are six basic methods for depositing patterned CP's (Holdcroft, 2001). Each of these was evaluated for their effectiveness and the ease with which the control electronics could be created.

Table 1. *Deposition Method Review.*

Technique	Issues
Electroless	Masking difficulties
Electrochemical	Requires conductive target
Selective Passivation	Residual stresses, masking difficulties
Printing (Microcontact or Screen)	Stamp fabrication, dynamic physical contact
Inkjet Printing	Lower conductivities of soluble CP's
Vapor Deposition	Not generally suitable for CP's

Table 1 summarizes the results of reviewing these deposition methods (further details in Wiedenman, 2008). While the organic vapor phase deposition (OVPD) technique was not generally suited to CP's, a variation of this process known as organic chemical vapor deposition (oCVD) can do so (Lock et al., 2006; Im et al., 2007). During the oCVD process, the CP is polymerized and deposited onto the target substrate in one straightforward step (see Figure 2). The oCVD process allows line-of-sight deposition without significant lateral migration, so the polymer can be patterned using a simple shadow mask. Additionally, oCVD is the most gentle process for the target substrate of all those examined. For these reasons, oCVD was the best method to deposit the control electronics in the current work. The CP poly(3,4-ethylenedioxythiophene) (PEDOT) was used in this work.

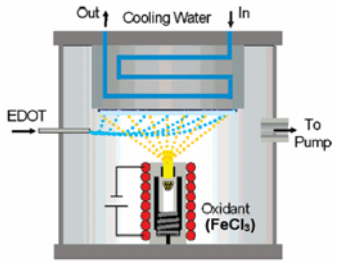

Figure 2. *In oxidative chemical vapor deposition (oCVD), the EDOT monomer flows in from the left, making contact with the sublimated oxidizing agent. Polymerization occurs, and the PEDOT deposits onto the target substrate. The target is held on the underside of a temperature-controlled platform at the top of the chamber (from Lock, 2006).*

Examination of the components fabricated using oCVD shows that the masking techniques used were effective. Scanning electron microscopy reveals the good definition of both the PEDOT and polystyrene (PS) layers (see Figure 3). The device depicted performed well on testing even though it was slightly contaminated with

unused oxidant (appearing as specks on the surface in the figure).

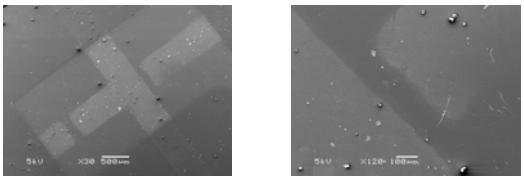

Figure 3. *The left figure shows an overview of a component deposited using oCVD. The PEDOT pattern is readily apparent, as is the polystyrene barrier layer over the outer portions of the device. The right figure shows a close-up of the gap of the same component, demonstrating the excellent definition of the PEDOT deposition achieved using wire EDM-fabricated masks.*

5. FEEDBACK ELECTRONIC COMPONENTS

In order to close the control loop in the device, a component is needed which will drive the error between the desired actuator strain and the actual strain of the device to zero. The simplest component for accomplishing this task is a differential amplifier (DA), which can be implemented with two transistors.

5.1 Previous Work

Many researchers have done work in the area of creating functional electronic components and devices using CP's. The first transistors incorporating CP's were fabricated in 1983 (Ebisawa et al., 1983) using polyacetylene as a semiconductor material in an organic field effect transistor (OFET). Continued research has led to the use of other CP's as channel materials (for example: Sirringhaus et al., 1998; and Horowitz, 2004) within silicon-based devices as well as progress towards fully organic components (Halik et al., 2002a and 2002b; Clemens et al., 2004).

Unfortunately, OFET's are currently impractical for a programmable material. The organic semiconductors used are very sensitive to surface morphology and therefore require deposition methods and patterning techniques that are too harsh to successfully deposit these components onto a PPy actuator backing. Simpler components are called for, such as electrochemical transistors.

Electrochemical transistors (ECT) are simply appropriately patterned traces of CP within an electrolyte. The electrolyte allows the establishment of electrochemical cells within the transistor, and the conductivity of the drain-source path can then be switched on and off electrochemically.

Early ECT work required immersion of the transistor in an electrolyte with an external counter electrode positioned adjacent (White et al., 1984; Kranz et al., 1995). As the ultimate goal is to create a programmable material that does not need to be immersed in electrolyte with a separate counter electrode nearby, ECT designs by Chen et al. were of great interest (Chen et al., 2002; Chen, 2005). These devices obviate the need for an external counter electrode through the use of two separate electrochemical cells.

5.2 Transistors

Chen's ECT were fabricated by first spin-coating a surface with a solution of PEDOT and poly(styrene sulfonic acid) (PSS). The patterns, shown in Figure 4, were made by scoring the surface with a plotter, removing the CP from unwanted areas. This technique is unsuited to the current application, but patterning these devices can be accomplished in an oCVD deposition using shadow masking.

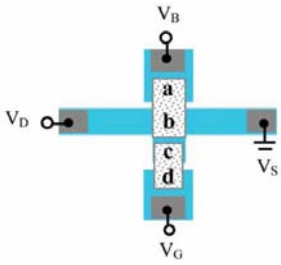

Figure 4. *Chen's design for a fully contained electrochemical transistor uses two electrolyte gel bridges at a-b and c-d to create two separate electrochemical cells. Modifying the gate voltage switches the conductivity of the drain-source path on and off (Chen, 2005).*

The bias voltage, $\boldsymbol{V_B}$ is maintained at a constant value (3.5 V in this case). For a zero gate voltage $\boldsymbol{V_G}$ and the source lead connected to ground, the ***a-b*** cell undergoes a redox reaction. Region ***a*** is oxidized while ***b*** is reduced, cutting off the drain-source conductive channel. This transistor is thus normally off. Increasing the gate voltage causes a similar redox reaction to occur in the ***c-d*** cell. However, in order for ***c*** to reduce, it must draw electrons from region ***b*** as there is no conductive path beyond ***b***. This effectively oxidizes ***b***, opening the conductive channel between drain and source. In this way the channel can be switched on by changing the gate voltage.

Using oCVD deposition of PEDOT and polystyrene, ECT's were fabricated. When tested, these ECT's demonstrated drain-source channel modulation as shown in Figure 5.

Based on these results, an empirical model of the drain-source channel resistance was derived for use in predicting the performance of integrated circuits containing these ECT's. For a constant drain-source voltage in the saturation region, the drain-source channel resistance $\boldsymbol{R_{ds}}$ is an exponential function of the gate-source voltage $\boldsymbol{V_{gs}}$:

$$R_{ds} = \left(6\times10^{6}\right)e^{-2.3V_{gs}} \qquad (6)$$

Transconductances of up to 1 mS were achieved with these components, though most were on the order of 0.1 mS. The ECT from Figure 5 has a transconductance of 0.046 mS and a threshold voltage of 1.7 V.

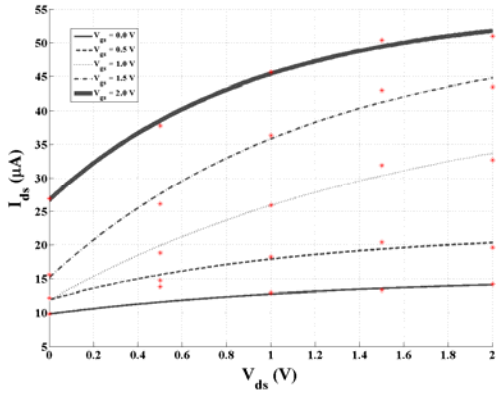

Figure 5. *After iterative improvement of the masking and deposition process, electrochemical transistors fabricated using oCVD demonstrated drain-source channel conductivity modulation.*

5.3 Differential Amplifiers

Electrochemical differential amplifiers (ECDA's) were fabricated using the oCVD process. Narrow conductive regions were used to implement the needed resistors. PS barrier material was deposited on all areas other than the test access pads and the two ECT, so that they might be open to the electrolyte.

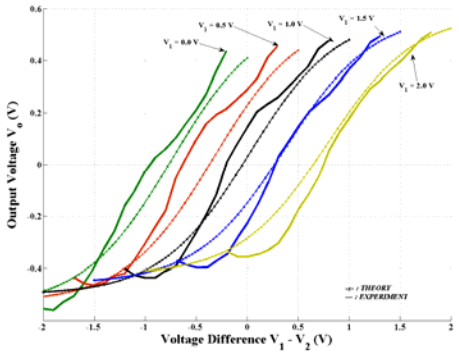

Figure 6. *The experimental and theoretical ECDA performances are shown side by side. With a constant DC offset removed from the theoretical results, the experimental data matches well.*

The resulting ECDA's were tested for their circuit performance. Using one input as the control and holding it constant while varying the other (treated as the sensor output signal), tests were conducted of the circuit behavior. These results are shown in Figure 6 along with the theoretical predictions. The theoretical predictions differed by a constant DC value from the experimental results, and this has been removed.

As can be seen, the theoretical predictions match the experimental results. Based on measured resistor characteristics of the experimental sample, an attenuation of 4.7 dB of the difference between V_1 and V_2 is expected and seen. This is the first operational electrochemical differential amplifier fabricated using the oCVD process.

Improvement of the ECDA performance can be accomplished through several means. Amplifications of up to 34 dB can be achieved through refinements to the deposition and masking process used to fabricate the device (Wiedenman, 2008).

6. SYSTEM INTEGRATION

6.1 Co-fabrication

The key to creating a programmable material is the co-fabrication of all the pieces in one seamless, integrated device. Vital to that co-fabrication is the deposition of the PS barrier layers. These were shown first to be sufficiently ionically and electronically insulative to prevent system shortouts by testing PEDOT samples that were both unmasked and masked with PS using cyclic voltammetric (CV) methods. The sample coated with PS showed significantly less activity than the bare PEDOT.

To examine the ability to deposit PPy electrochemically using vapor deposited PEDOT as a working electrode, samples were fabricated with PEDOT deposited via oCVD onto polyethylene terephthalate (PET) and PPy. To determine the appropriate voltage for the ECD, CV tests were conducted with and without pyrrole monomer in solution.

ECD was carried out under TBAP/PC conditions and PPy was successfully deposited. Unfortunately, the PC-based electrolyte damaged the PS layer, causing separation of the PPy substrate and the newly deposited PPy layer.

This was remedied in a later co-fabrication test using an aqueous solution. Even though the deposition had to take place at a higher temperature (4°C rather than the -40°C used with PC electrolyte), the deposition was successful (Wiedenman, 2008).

6.2 System Model

Having demonstrated that the fabrication methodology for constructing the programmable material is feasible, it is now necessary to synthesize the previous mathematical component models into an overall system theoretical construct. This model incorporates the experimentally verified representations of the actuator, sensor, and control electronics.

The integrated system can be represented as a lumped parameter model as shown in Figure 7. The actuator

consists of a resistance in series with a capacitance and diffusion impedance in parallel (J. Madden, 2000). The sensor resistor is shown as one leg of a Wheatstone bridge configuration. The electrochemical transistors are embedded within the differential amplifier, which receives the desired input signal, V_d, and the sensor output, V_b, and outputs a control voltage. This output voltage directs the flow of current from a bipolar source through two transistors, which provides the current to drive the actuator.

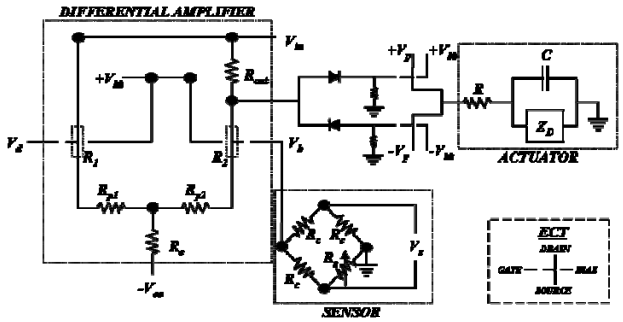

Figure 7. *In this lumped parameter model, the actuator has been modeled as a resistance (representing the electrolyte/contact resistance) in series with a capacitor (representing the double layer capacitance) in parallel with the diffusion impedance (J. Madden, 2000). The electrochemical differential amplifier is shown to the left, and the Wheatstone bridge containing the sensor variable resistor is shown to the lower right. A pair of transistors is used between the amplifier and the actuator to provide the necessary driving current.*

The previously derived mathematical representations of the constituent components of the programmable material were synthesized into a predictive model. Based on this integrated model, currently available ECT performance, and easily achievable improvements in resistor precision, testable predictions of the system performance are made. The overall system response time is limited primarily by the actuator. The 19 second settling time of the actuator is lengthened slightly by the electrochemical activation times of the transistors, but the actuator response is still by far the slowest component of the system response.

A 1 MPa step stress input results in a mechanical strain response (ε_m) of 1.61% before creep effects set in. This mechanical response is what the programmable material would experience in the absence of any feedback behavior. The charge-driven strain (ε_q) reaches 0.26% after the actuator settling time. This gives a resultant strain (ε_r) of approximately 1.35% (see Figure 8). This resultant strain causes the apparent stiffness of the programmable material to increase over the unactuated stiffness of the PPy layers comprising the bulk of the device. The ratio of the apparent stiffness to the unactuated stiffness, termed K_E, is 1.18 in this case (as shown in Figure 8 inset).

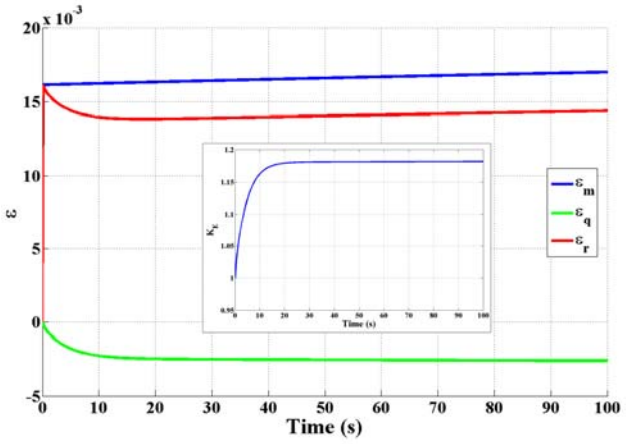

Figure 8. *This plot shows the system response for a 1 MPa stress step input. The mechanical strain, ε_m, is offset by the charge driven strain, ε_q, to give a resultant strain of ε_r. The programmable material increases the apparent stiffness by 18% (inset).*

CONCLUSIONS

This work is the beginning of a quest to create a device which closely replicates the behavior and performance of mammalian skeletal muscle. This remarkable actuation device has intricately co-fabricated and integrated actuation, sensory, control, and energy delivery capabilities that have resulted from millions of years of evolution. This research has conceptualized a device, known as a programmable material, which integrates many of these same capabilities and co-fabricates them in such a way as to appear externally to be a single homogeneous material.

CP actuators, sensors, and control electronics have all been fabricated in such a manner that they may be co-fabricated into an integrated device. Co-fabrication has been demonstrated, an integrated system model has been devised, and predictions have been made about the performance of a fully-realized programmable material.

The complete fabrication of a programmable material remains to be done. Many of the preliminary issues confounding this effort have been resolved in this work, but problems remain to be solved before full implementation.

Successful implementation of a programmable material may lead to embeddable controlled actuation devices. These could be utilized by a soldier as part of a functionalized uniform to minimize muscle jitter during precision individual targeting, as an on-call or automatic tourniquet, or as part of an adjustable flexibility individual armor system. There is significant potential for a programmable material to be implantable in the human body, where it may someday supplement existing muscle strength or replace muscle capability otherwise lost.

ACKNOWLEDGEMENTS

The authors wish to thank the Institute for Soldier Nanotechnologies at the Massachusetts Institute of Technology for its continued support of this research. Thanks especially to Professor Karen Gleason, who graciously allowed use of her laboratory facilities for the oCVD work. MAJ Wiedenman further thanks the Uniformed Army Scientist and Engineer program for providing him the opportunity to conduct this research as part of his doctoral studies.

REFERENCES

Anquetil, P. A., D. Rinderknecht, N. A. Vandesteeg, J. Madden, and I. W. Hunter, 2004: Large Strain Actuation In Polypyrrole Actuators. *Proceedings of SPIE*, 5385 (Smart Structures and Materials 2004 - Electroactive Polymer Actuators and Devices (EAPAD)).

Chen, A., 2006: Large Displacement Fast Conducting Polymer Actuators. *M.S. thesis, Massachusetts Institute of Technology.*

Chen, M. X., 2005: Printed Electrochemical Devices Using Conducting Polymers As Active Materials On Flexible Substrates. *Proc. IEEE*, **93**, 1339-1347.

Chen,M. X., D. Nilsson, T. Kugler, M. Berggren, and T. Remonen, 2002: Electric Current Rectification By An All-Organic Electrochemical Device. *Appl. Phys. Lett.*, **81**, 2011-2013.

Clemens, W., I. Fix, J. Ficker, A. Knobloch, and A. Ullmann, 2004: From Polymer Transistors Toward Printed Electronics. *J. Mat. Res.*, **19**, 1963-1973.

Ebisawa, F., T. Kurokawa, and S. Nara, 1983: Electrical-Properties of Polyacetylene Polysiloxane Interface. *J. Appl. Phys.*, **54**, 3255-3259.

Halik, M., H. Klauk, U. Zschieschang, T. Kriem, G. Schmid, W. Radlik, and K. Wussow, 2002a: Fully Patterned All-Organic Thin Film Transistors. *Appl. Phys. Lett.*, **81**, 289-291.

Halik, M., H. Klauk, U. Zshieschang, G. Schmid, W. Radlik, and W. Weber, 2002b: Polymer Gate Dielectrics And Conducting-Polymer Contacts For High-Performance Organic Thin-Film Transistors. *Adv. Mat.*, **14**, 1717-1722.

Hara, S., T. Zama, W. Takashima, and K. Kaneto, 2006: Tris(triuoromethylsulfonyl) Methide-Doped Polypyrrole As A Conducting Polymer Actuator With Large Electrochemical Strain. *Synth. Met.*, **156**, 351-355.

Holdcroft, S., 2001: Patterning Pi-Conjugated Polymers. *Adv. Mat.*, **13**, 1753-1765.

Horowitz, G., 2004: Organic Thin Film Transistors: From Theory To Real Devices. *J. Mat. Res.*, **19**, 1946-1962.

Im, S. G., K. K. Gleason, and E. A. Olivetti, 2007: Doping Level And Work Function Control In Oxidative Chemical Vapor Deposited Poly (3,4-ethylenedioxythiophene). *Appl. Phys. Lett.*, **90**.

Kranz, C., M. Ludwig, H. E. Gaub, and W. Schuhmann, 1995: Lateral Deposition of Polypyrrole Lines Over Insulating Gaps - Towards The Development Of Polymer-Based Electronic Devices. *Adv. Mat.*, **7**, 568-571.

Lock, J. P., S. G. Im, and K. K. Gleason, 2006: Oxidative Chemical Vapor Deposition Of Electrically Conducting Poly(3,4-Ethylenedioxythiophene) Films. *Macromol.*, **39**, 5326-5329.

Madden, J. D., 2000: Conducting Polymer Actuators. *Ph.D. thesis, Massachusetts Institute of Technology*.

Madden, J. D. W., N. A. Vandesteeg, P. A. Anquetil, P. G. A. Madden, A. Takshi, R. Z. Pytel, S. R. Lafontaine, P. A. Wieringa, and I. W. Hunter, 2004: Artificial Muscle Technology: Physical Principles And Naval Prospects. *IEEE J. Oc. Eng.*, **29**, 706-728.

Madden, P. G., J. D. Madden, P. A. Anquetil, H. Yu, T. M. Swager, and I. W. Hunter, 2001: Conducting Polymers As Building Blocks For Biomimetic Systems.

Madden, P. G. A., 2003: Development And Modeling Of Conducting Polymer Actuators And The Fabrication Of A Conducting Polymer Based Feedback Loop. *Ph.D. thesis, Massachusetts Institute of Technology.*

Pytel, R. Z., 2007: Artificial Muscle Morphology – Structure / Property Relationships in Polypyrrole Actuators. *Ph.D. thesis, Massachusetts Institute of Technology.*

Sirringhaus, H., N. Tessler, and R. H. Friend, 1998: Integrated Optoelectronic Devices Based On Conjugated Polymers. *Science*, **280**, 1741-1744.

Smela, E., 1999: Microfabrication of PPy Microactuators and Other Conjugated Polymer Devices. *J. Micromech. Microeng.*, **9**, 1-18.

Vandesteeg, N. A., 2007: Synthesis And Characterization Of Conducting Polymer Actuators. *Ph.D. thesis, Massachusetts Institute of Technology.*

White, H. S., G. P. Kittlesen, and M. S. Wrighton, 1984: Chemical Derivatization Of An Array Of 3 Gold Microelectrodes With Polypyrrole - Fabrication Of A Molecule- Based Transistor. *J. Am. Chem. Soc.*, **106**, 5375-5377.

Wiedenman, N. S., 2008: Towards Programmable Materials: Tunable Material Properties Through Feedback Control of Conducting Polymers. *Ph.D. thesis, Massachusetts Institute of Technology.*

Yamaura, M., T. Hagiwara, and K. Iwata, 1988: Enhancement of Electrical Conductivity Of Poly-Pyrrolefilm By Stretching - Counter Ion Effect. *Synth. Met.*, **26**, 209-224.